Mechanical loading of mouse caudal vertebrae increases trabecular and cortical bone mass-dependence on dose and genotype

Webster, D ; Wasserman, E ; Ehrbar, M ; Weber, Franz E ; Bab, I ; Müller, R

Abstract: Most in vivo studies addressing the skeletal responses of mice to mechanical loading have targeted cortical bone. To investigate trabecular bone responses also we have developed a caudal vertebral axial compression device (CVAD) that transmits mechanical loads to compress the fifth caudal vertebra via stainless steel pins inserted into the forth and sixth caudal vertebral bodies. Here, we used the CVAD in C57BL/6 (B6) and C3H/Hej (C3H) female mice (15 weeks of age) to investigate whether the effect of regular bouts of mechanical stimulation on bone modeling and bone mass was dependent on dose and genotype. A combined micro-computed tomographic and dynamic histomorphometric analysis was carried out at the end of a 4-week loading regimen (3,000 cycles, 10 Hz, 3 x week) for load amplitudes of 0N, 2N, 4N and 8N. Significant increases in trabecular bone mass of 9 and 21% for loads of 4N and 8N, respectively, were observed in B6 mice. A significant increase of 10% in trabecular bone mass occurred for a load of 8N in the C3H strain. For other loads, no significant increases were detected. Both mouse strains exhibited substantial increases in trabecular bone formation rates for all loads, B6: 111% (2N), 86% (4N), 164% (8N), C3H: 41% (2N), 38% (4N), 141% (8N). Significant decreases in osteoclast number of 146 and 93% for a load of 8N were detected in B6 and C3H mice, respectively. These findings demonstrate that the effect of loading on the structural and functional parameters of bone is dose and genotype dependent. The caudal vertebral loading model established here is proposed for further studies addressing the molecular processes involved in the skeletal responses to mechanical stimuli.

DOI: https://doi.org/10.1007/s10237-010-0210-1

Mechanical Loading of Mouse Caudal Vertebrae Increases Trabecular and Cortical Bone Mass – Dependence on Dose and Genotype

Duncan Webster[1], Elad Wasserman[1,2], Martin Ehrbar[2], Franz Weber[3], Itai Bab[2], Ralph Müller[1*]

[1]Institute for Biomechanics, ETH Zürich, Zürich, Switzerland. [2]Bone Laboratory, The Hebrew University of Jerusalem, Jerusalem, Israel. [3]Department of Craniomaxillofacial Surgery, University of Zürich, Zürich, Switzerland.

* Corresponding Author

Prof. Dr. Ralph Müller

ETH Zürich

Institute for Biomechanics

Wolfgang-Pauli-Strasse 10

8093 Zürich, Switzerland

tel/fax +41.44.632.4592/1214

http://www.biomech.ethz.ch

Abstract

Most *in vivo* studies addressing the skeletal responses of mice to mechanical loading have targeted cortical bone. To investigate trabecular bone responses also we have developed a caudal vertebral axial compression device (CVAD) that transmits mechanical loads to compress the fifth caudal vertebra via stainless steel pins inserted into the forth and sixth caudal vertebral bodies. Here we used the CVAD in C57BL/6 and C3H/Hej mice to investigate whether the effect of regular bouts of mechanical stimulation on bone remodeling and bone mass were dependent on dose and genotype. A combined micro-computed tomographic and dynamic histomorphometric analysis carried out at the end of a 4-week loading regimen for load amplitudes of 0N, 2N, 4N and 8N revealed that an amplitude of 8N stimulated significant increases in trabecular and cortical bone mass mainly in the C57BL/6 strain. Both biological strains exhibited substantial increases in bone formation rates and decreases in osteoblast number. These findings demonstrate that the effect of loading on the structural and functional parameters of bone is dose- and genotype dependent. The caudal vertebral loading model established here is proposed for further studies addressing the molecular processes involved in the skeletal responses to mechanical stimuli.

Key words

Mechanical loading, trabecular bone, cortical bone, bone adaptation, bone histomorphometry

Introduction

Mechanical loading, is perhaps the most important environmental determinant of bone mass and functional integrity. It is well established that insufficient mechanical stimuli, as in the case of prolonged bed rest and hypogravity, lead to massive bone loss. Conversely it has also been demonstrated that mechanical overloading results in enhanced bone formation and a net gain in bone mass (1-4). These stimuli affect both cortical and trabecular bone in particular trabecular bone which has been shown to have a more enduring sensitivity to mechanical stimulation in human adults (5,6). Osteoporosis, the most prevalent degenerative disease in western societies, has been partly attributed to a reduction in muscle mass and function and consequently decreased mechanical usage of the skeleton (7). Hence, it is anticipated that an understanding of the processes involved in the skeletal response to mechanical forces could lead to the identification of molecular targets for the development of anti-osteoporotic therapies.

The availability of in vivo models for load regulated bone adaptation is key to understanding the underlying biochemical mechanisms. To study cortical bone several studies have established in vivo mouse models which demonstrate significant increases in bone formation in response to dynamic load regimens at tibial sites (8-10). These models have been used to investigate the biochemical pathways associated with load-induced cortical bone adaptation using C57BL/6 and C3H/Hej inbred strains (11-13). These strains are of particular interest as they exhibit a number of contrasting phenotypes specific to both cortical and trabecular bone, including the mechano-sensitivity of cortical bone (8,14-16). Furthermore breeding strategies have been employed together with quantitative trait loci (QTL) analysis in an effort to refine the search for the chromosomal regions responsible for the complementary phenotypes (17,18). However specific genes and or combinations of genes which regulate load induced bone adaptation have yet to be discovered. Compared to cortical bone, trabecular bone

has been studied less extensively. One of the few models currently available to assess load induced changes in trabecular bone uses a mechanical device to apply an axial compressive force to the 8th caudal vertebrae of a rat via K-wires inserted into the two, adjacent caudal vertebrae (19,20) . However, studies employing this model have been hampered by the current inaccessibility to genetic manipulations, which are available mainly in mice. Two studies have reported load induced trabecular bone adaptation in mice. De Souza et al (21) mechanically stimulated mice tibia using dynamic loads with magnitudes between 5 and 13 N and demonstrated a significant increase in trabecular bone volume density when pooling all the loaded groups together. Using a similar approach Fritton et al (22) showed trabecular bone volume density and trabecular thickness to increase significantly by 15 % and 12 % when applying a single 6 week long loading regimen. Here we present an alternative in vivo model for the study of both cortical and trabecular bone adaptation. Using an approach similar to the rat vertebra model we hypothesize that the response of murine cortical and trabecular bone to mechanical loading is both dose and genotype dependent. The objectives of this study are therefore twofold: 1) To show that the caudal vertebrae of B6 and C3H mice can be mechanically stimulated in a similar manner to that performed in rats (19) and 2) To compare the skeletal responsiveness to mechanical stimulation in both B6 and C3H mouse strains.

Materials and methods

Mechanical loading apparatus

To mechanically load murine vertebrae a dual-axis closed-loop feedback device was used. This device has been developed to apply a precisely controlled cyclical, compressive load to the fifth caudal vertebrae (C5) of mice at a frequency of 10Hz via stainless steel pins surgically inserted into the fourth (C4) and sixth caudal (C6) vertebrae (Fig. 1). For more information refer to the

previous publication which details the validation of the device (23). As a quality control, the feedback signal from the load cell was recorded and all force maxima and minima determined. Surgical insertion of the stainless steel pins was performed using a special pinning device, compatible with X-ray fluoroscopy. The device makes use of a V-clamp to simultaneously secure and automatically locate the cranio-caudal axis of the mouse tail. The pins are loaded into channels integral to the V-clamp and are manually pushed through the centers of the vertebrae, perpendicular to the cranial-caudal axis. A digital mobile C-arm (OEC MiniView 6800, GE Medical Systems, Glattbrugg, Switzerland) was used to locate C4 and C6 for pinning.

Experimental design

Female mice, 40 B6 and 40 C3H, 9 weeks of age (Harlan Ltd.) were housed in a husbandry unit in groups of 5 and given 3 weeks to acclimatize to their new environment. Then, all mice had stainless steel insect pins (0.5mm diameter, Fine Science Tools, Heidelberg, Germany) surgically inserted into their C4 and C6 vertebrae and given 3 weeks to recover before loading commenced. For loading, the mice were divided into 8 loading groups (n =10): $B6_{0N/\ 2N/\ 4N/\ 8N}$ and $C3H_{0N/\ 2N/\ 4N/\ 8N.}$ $B6_{0N}$ and $C3H_{0N}$ formed the sham groups whilst the remaining groups were submitted to an intensive loading regime whereby sinusoidally varying forces (3000 cycles, 10Hz) were applied to all C5's with amplitudes corresponding to the group subscript. This was repeated 3 times a week for a duration of 4 weeks. To vitally label newly formed bone 100 ml of the fluorochrome calcein (Sigma, 15mg/Kg) was administered intraperitonally 4 days and 1 day prior to sacrifice. To protect the structural integrity of the pinned vertebrae, sudden impulses were avoided by linearly increasing the force at a rate of 1 Ns^{-1} until the peak force was attained at which point the dynamic signal was applied. At 19 weeks of age, following 4 weeks of loading all mice were sacrificed using C02 inhalation. Upon sacrifice of the mice the C5's were harvested and

immediately fixed in formalin for 48 hours, after which they were transferred to saline containing 70% ethanol. Throughout pin insertion and loading the mice were anesthetized using an oxygen-isoflurane mixture (Provet Medical AG, Lyssach, Switzerland). To monitor the health of the mice, each mouse was weighed prior to loading and after each loading bout. The accuracy of the CVAD was assessed by analyzing the recorded force feedback signals for each loading bout and for each mouse to determine each peak and minimum force value present in the applied dynamic signals. All animal procedures were approved by the local animal ethics committee (Kantonales Veterinäramt Zürich, Zürich, Switzerland)

Quantification of bone adaptation

Bone morphometry was assessed using micro-computed tomography (micro-CT) with 5 times frame averaging (6 µm voxel size, 50 kVp, 160µA, Scanco Medical AG, Basserdorf, Switzerland) to obtain 3D, digital images of all C5 vertebrae. Using a direct 3D approach (24) morphometric parameters specific to trabecular and cortical bone were determined for a global volume these included: Trabecular bone volume density (BV/TV_{Tb}), trabecular bone volume (BV_{Tb}), trabecular tissue volume (TV_{Tb}), trabecular thickness (Tb.Th), trabecular number (Tb.N), cortical bone volume density (BV/TV_{Ct}), cortical bone volume (BV_{Ct}), cortical tissue volume (TV_{Ct}), cortical thickness (Ct.Th) and marrow volume (MV). Global trabecular and cortical volumes were defined by adapting an algorithm developed earlier (25) to automatically isolate the outer volume, cortical bone and an internal volume comprised of spongiosa, both primary and secondary (trabecular bone). Primary spongiosa was then excluded from analysis by discarding distal and proximal sub-volumes to ensure only trabecular bone remained (Fig. 2A). For B6 mice each of these two regions measured 10% of the total height of the total, isolated volume. Owing to the presence of more distal primary spongiosa in C3H mice the discarded distal and proximal

regions measured 10% and 15% respectively. The global cortical region of analysis was similarly defined such that it was comprised of the cortical shell enclosing the global trabecular volume. Where global analysis failed to detect a significant load induced anabolic effect local analyses were performed. This was executed by subdividing both cortical and trabecular global volumes into overlapping regions each having a height equal to 10% of the total height of the volume originally isolated (containing both primary and secondary spongiosa). For B6 mice this resulted in 15 overlapping regions (Figs. 2B & C). Similarly for C3H mice this resulted in 14 overlapping regions. Histomorphometric indices for trabecular and cortical regions were quantified using histological techniques for trabecular (Tb), periosteal-cortical (Pe) and endosteal-cortical (En) surfaces. Both single labelled (sLS) and doubled labelled (dLS) surfaces were measured the sum of which was used to determine the mineralized perimeter of bone: $Md.Pm_{Tb/Pe/En}$ (a surrogate of osteoblast number). Mineral appositional rate ($MAR_{Tb/Pe/En}$: a surrogate of osteoblast activity) was also obtained by dividing the average distance between the double labels on the bone surfaces by the number of days between injections. In addition bone formation rates ($BFR_{Tb/Pe/En}$), were determined by multiplying the sum of sLS and dLS by MAR. To permit inter-strain comparison Md.Pm and BFR were normalized by total bone surface perimeter (Pm) to give Md.Pm/Pm and BFR/Pm. All indices were determined from 3 single histological slices taken from the mid-sagittal plane of each double labelled vertebra according to the standards in histomorphometry (26). Tartrate Resistant Acid Phosphatase (TRAP) staining was also performed on adjacent sections to measure the number of osteoclasts present per unit of trabecular perimeter ($N.Oc/Pm_{Tb}$).

Statistical analysis

A Students T-test was used to compare the base line morphological parameters specific to both biological strains. To investigate the effect of mechanical loading on each strain, ANOVA was used to compare global CT-measured morphometric parameters and dynamic histomorphometric parameters for each loading group. Where significance was detected post-hoc pair wise T-tests with bonferroni corrections were used to determine the significance of the differences relative to the 0N loading groups. In the cases where global micro-CT analysis failed to detect a load induced anabolic effect repeated measures anova with the necessary Bonferroni corrections was used to compare the different regions and assess the local effects of loading specific to each mouse strain, yielding a group-region interaction p-value (P_{int}). To compare the relative mechano-sensitivity of the two biological strains, two-way ANOVA was used to contrast their dose responses as measured by both micro-CT and histomorphometry. Owing to the difference in bone size between the two strains the micro-CT measured dose responses were first normalized using their respective 0N loading groups. Again where significance was detected post-hoc pair-wise T-tests with Bonferroni corrections were used to determine the significance of inter-strain differences at different loads. Regional effects were not compared between mouse strains. For all statistical analyses, the GNU statistical package R (Version 2.5.1, http://www.r-project.org) was used. Results were considered statistically significant for adjusted P-values lower than 0.05.

Results

Throughout the duration of the experiment no mice were lost due to death and the average weights of the mice throughout loading did not decrease, suggesting that the general health of each mouse remained satisfactory. Analysis of the recorded force feedback signals for each loading bout and for each mouse demonstrates the high accuracy at which the CVAD controls the

user defined force. The average force amplitudes applied during the entire experiment were 2.02N ± 0.01 N and 4.03 ± 0.02N and 8.06 ± 0.07N.

Trabecular bone

The mean baseline global parameters for trabecular bone as measured by the $B6_{0N}$ and $C3H_{0N}$ loading groups are shown in Table 1. Compared to the C3H strain these data show that in the absence of mechanical loading mean global trabecular bone volume and trabecular number are 110% (0.32 mm^3) and 48% (0.96 mm^{-1}) higher for the B6 strain respectively ($P < 0.0001$) whilst mean global trabecular thickness is 16% (14.9 μm) lower. These data can be considered to be representative of normal B6 and C3H populations as previous pilot studies have shown pinning of C4 and C6 caudal vertebrae to have a negligible effect on the typical morphology of C5 vertebrae for both trabecular and cortical bone.

When comparing the micro-CT data sets for all B6 loading groups Anova detected highly significant changes in global BV/TV_{Tb}, BV_{Tb} and Tb.Th ($P < 0.001$). No significant differences were detected for global TV_{Tb}, and Tb.N ($P > 0.1$). Comparison of $B6_{8N}$ and $B6_{0N}$ groups shows global BV/TV_{Tb} and BV_{Tb} to increase by 26% (Table 1, Fig. 3A) and 29% (0.18 mm^3) respectively ($P < 0.001$). No significant changes were observed in global TV_{Tb}. Analysis of the global structural indices show the increase in bone mass to correspond to a 22% increase (16.9μm, $P < 0.001$) in Tb.Th and a non-significant 3 % increase (0.09 mm^{-1}, $P > 0.5$) in Tb.N. Regional comparison of BV/TV_{Tb}, BV_{Tb} and Tb.Th for the $B6_{0N}$ and $B6_{8N}$ loading groups confirms the reported, global anabolic effect. Furthermore significant local increases of up to 14.56% (0.69 mm^{-1}) are observed for Tb.N (Fig. 3B), $P_{int} < 0.01$. No significant global differences were detected when comparing $B6_{2N}$ and $B6_{4N}$ groups with the 0N loading group. Significant local increases in BV_{Tb}, of up to 26 % (0.025 mm^3), were detected when comparing

$B6_{4N}$ and $B6_{0N}$ ($P_{int} < 0.05$). No other significant local increases were observed. The effect of mechanical stimulation on the trabecular component of bone can be clearly seen (Fig. 4).

When comparing the histological data sets for all B6 loading groups Anova detected significant differences for mineralizing perimeter ($Md.Pm/Pm_{Tb}$) and bone formation rate (BFR/Pm_{Tb}). $Md.Pm/Pm_{Tb}$ was found to increase significantly by 72% (21.2 mm/mm $x10^{-2}$) for the group loaded at 2N, by 64% (18.7 mm/mm $x10^{-2}$) when loaded at 4N and by 89% (26.1 mm/mm $x10^{-2}$) when loaded at 8N, ($P < 0.05$; Fig.5A). A similar but non-significant trend was reported for MAR_{Tb}. Increases of 36% (0.55 μm/day) and 29% (0.45 μm/day) were observed for loads of 2N and 4N respectively ($P > 0.2$), whilst an almost significant 56% (0.86 μm/day) was reported for a load of 8N ($P = 0.051$; Fig. 5B). Significant increases in bone formation rate of 54% (109 $\mu m^3/\mu m^2$/day $x10^{-2}$) and 82% (163 $\mu m^3/\mu m^2$/day $x10^{-2}$) were reported for $B6_{2N}$ and $B6_{8N}$ groups only ($P < 0.01$), with a near significant increase of 43% (86.5 $\mu m^3/\mu m^2$/day) being shown for $B6_{4N}$ ($P = 0.06$). The Osteoclast number per perimeter was shown to significantly decrease for groups loaded at 2N and 8N by 71% (1.57 mm^{-1}) and 52% (1.15 mm^{-1}) respectively ($P < 0.05$) with non-significant reduction of 35% (0.77 mm^{-1}) being reported for 4N ($P > 0.2$).

When comparing all loading groups for the C3H strain Anova detected significant differences for global BV/TV_{Tb} ($P < 0.05$). Comparison of the $C3H_{8N}$ and $C3H_{0N}$ shows global BV/TV_{Tb} to be increased, almost significantly, by 14.22% ($P = 0.055$; Fig. 3A) owing to a 13.5% (0.039 mm^3, $P < 0.2$) increase in global BV_{Tb} and a non significant decrease in global TV_{Tb} (Table 1). Global Tb.Th and Tb.N were shown to increase non-significantly by 7.62% (7 μm) and 2.49% (0.058 mm^{-1}) respectively. Local analysis revealed significant group-region interaction terms for BV/TV_{Tb} and BV_{Tb} when comparing $C3H_{8N}$ and $C3H_{0N}$. BV/TV_{Tb} was shown to increase by up to 31% ($P_{int} < 0.01$; Fig. 3C) whilst BV_{Tb} was show to increase by up to 32% (0.026 mm^3, $P_{int} < 0.01$). The maximum reported increases in Tb.Th and Tb.N were 14.7% (11.7

μm) and 4.87% (0.11 mm^{-1}) respectively, (P_{int} > 0.5). Comparison of the other loading groups with the $C3H_{0N}$ group yielded no significant global or regional differences. Analysis of the histomorphometric indices shows that a significant 48% (27.7 mm/mm $x10^{-2}$) increase in $Md.Pm/Pm_{Tb}$ was found for the $C3H_{8N}$ group only ($P < 0.05$; Fig. 5A). Significant 15% (0.19μm/day) and 41% (0.50μm/day) increases in MAR_{Tb} are observed in $C3H_{4N}$ and $C3H_{8N}$ loading groups respectively ($P < 0.05$; Fig. 5b). This however, only translates to a significant 110% (0.78 $\mu m^3/\mu m^2$/day $x10^{-2}$) increase in BFR_{Tb} for $C3H_{8N}$ ($P < 0.01$; Fig. 5C). Significant changes in osteoclast number were also observed. For loads of 2N, 4N and 8N osteoclast number decreased significantly by 59% (2.59 mm^{-1}), 73% (3.21 mm^{-1}) and 77% (3.40 mm^{-1}), respectively ($P < 0.01$).

Inter-strain comparison of the trabecular global components shows that global percentage increases in BV/TV_{Tb}, BV_{Tb}, are significantly higher for the B6 strain when loaded at 4N and 8N. The percentage increase in global BV/TV_{Tb} is shown to be 575% and 296% higher for the B6 strain for loads of 4N and 8N respectively ($P < 0.05$; Fig. 3A), likewise global percentage increases in BV_{Tb} are 1998% (0.05 mm^3) and 322% (0.14 mm^3) for loads of 4N and 8N respectively. Global percentage increases in Tb.Th are significantly higher for the B6 strain (394%, 10.1 μm, $P < 0.05$) for a load of 8N only. No significant differences are reported for global percentage increases in Tb.N and TV_{Tb}. Furthermore no significant differences occur in any parameter for an applied load of 2N. $Md.Pm/Pm_{Tb}$ is shown to be consistently higher for the C3H strain, significantly so for loads of 2N and 8N. Conversely MAR_{Tb} is shown to be consistently higher for the B6 strain, however this is only shown to be statistically significant for a load of 2N (Fig. 5B). No significant differences exist between strains when comparing BFR/Pm_{Tb} (Fig. 5C).

Cortical bone

Table 1 shows that unloaded C3H C5 vertebrae possess significantly more cortical bone mass resulting in a thicker cortical shell and larger cross sectional area. When comparing global cortical parameters for all B6 loading groups anova detected a significant difference for BV_{Ct} only ($P < 0.05$). Comparison of the $B6_{8N}$ group with the $B6_{0N}$ group showed global BV_{Ct} to be 11% (0.22mm^3) higher ($P = 0.058$; Fig. 6A). Global Ct.Th was shown to increase by 5.44% (7 µm, $P > 0.2$), TV_{Ct} by 5.9% (0.32 mm^3, $P > 0.2$) and MV by 3.01% (0.11 mm^3, $P > 0.2$). Localized anabolic effects were detected however. Regional analysis yielded significant group-region interaction terms for both BV/TV_{Ct} and BV_{Ct} when comparing $B6_{8N}$ and $B6_{0N}$ ($P_{int} < 0.001$). BV/TV_{Ct} and BV_{Ct} are shown to increase by up to 11.2% and 17.6% (0.04 mm^3; Fig. 6B) when loaded at 8N. This corresponded to non-significant regional increases of up to 9% (11 µm) for Ct.Th, 8.3% (0.05 mm^3) for TV_{Ct} and 7.9% (0.022 mm^3) for MV, ($P_{int} > 0.5$). No significant differences were detected when comparing both global and local parameters for the other loading groups. Histology shows no significant differences to exist between loading groups for Md.Pm/Pm at periostial cortical sites (Fig. 5A). The mineralized perimeter is however much greater at endostial cortical sites, where a significant 57% (28.4 mm/mm x10^{-2}) increase is reported for the $B6_{8N}$ loading group ($P < 0.01$). Owing to the absence of double calcein labels at periostial-cortical sites in the $B6_{0N}$ group MAR_{Pe} and BFR_{Pe} are shown to be greater for all other loading groups, however none of the reported increases are significantly different to $B6_{0N}$ (Figs. 5B & C). No Significant differences were detected for Mineral Apposition Rate at endostial cortical sites. Bone formation Rate is however shown to be significantly higher for a load of 8N at endostial cortical sites by 123% (0.86 µm^3/ µm^2/day x10^{-2}; Fig. 5C).

When comparing loading groups for the C3H strain anova found no significant differences for any global or local parameter, as measured by micro-CT (Fig. 6A). Analysis of

the histomorphometric indices shows the mineralized perimeter to increase at periostial-cortical sites with increasing load (Fig. 5A) however the only significant increase is that reported by $C3H_{8N}$ (233%, 37.56 mm/mm $x10^{-2}$, $P< 0.05$). No significant increases with load are reported in mineralized perimeter at endostial-cortical sites. Comparison of $C3H_{0N}$ and $C3H_{8N}$, shows mineral apposition rate at periostial-cortical sites to increase almost significantly by 65% (0.81 μm/day, $P = 0.06$), which translates into a significant 371% (0.84 $\mu m^3/ \mu m^2$/day $x10^{-2}$) increase in BFR_{Pe} ($P < 0.05$). Both MAR and BFR at endostial-cortical sites show significant 34% (0.44 μm^2/day) and 76.8% (0.57 $\mu m^3/ \mu m^2$/day $x10^{-2}$) increases for an applied load of 8N respectively, significant values are also reported for a load of 2N.

Inter-strain comparison shows that no significant global differences exist for BV/TV_{Ct}, however the percentage increase in global BV reported in the B6 strain is significantly different to that of the C3H strain (Fig. 6A). Whilst micro-CT shows actual 3D adaptation to be greater for the B6 mice, histomorphometry shows activity to be significantly higher in the C3H strain for periostial cortical surfaces. $Md.Pm/Pm_{Pe}$, MAR_{Pe} and BFR/Pm_{Pe} are all greater for the C3H strain, significantly so in all cases apart from MAR when loaded at 4N (Figs. 5A, B & C). No significant inter-strain differences exist for any of the histological parameters at Endosteal-cortical sites.

Discussion

In this study we hypothesized that load induced cortical and trabecular bone adaptation is both dose and genotype dependent. With respect to the first hypothesis, the significant global increase in trabecular BV/TV for a load of 8N combined with the significant local increases in trabecular BV/TV for a load of 4N confirms a dose dependency for trabecular bone in B6 mice. Analysis of the other structural parameters for the 8N group infers that the global increase in bone volume

density can be attributed to both the thickening of existing trabeculae and the formation of new trabeculae, demonstrating that a fully anabolic model has been established. For a load amplitude of 4N, no significant changes in any structural parameter accompanied the regional increases detected in bone mass, i.e. trabecular thickness. However, this could be explained by the magnitude of change being smaller than the 6 micron resolution of the imaging system. Trabecular dose dependency was not inferred by histomorphometry. Whilst the elevated values of Md.Pm/Pm, MAR and the significant increase in BFR concur with micro-CT data for a load amplitude of 8N, the relative increases reported by the 2N and 4N loading groups do not reflect the dose dependency as described by micro-CT. All dynamic indices for 2N and 4N are similar, yet only regional significant changes were detected in 3-dimensions for the 4N loading group. These data may allude to a lag in the remodelling process for a load of 2N, suggesting that if loading was to continue similar 3-dimensional geometric changes would start to occur in the 2N loading group. This observation hints at a mechanism which is dependent on the cumulative amount of mechanical energy transferred to the bone matrix i.e. fatigue induced micro-cracks (27,28).

To our knowledge this is the first time a dose response has been demonstrated in loaded, murine trabecular bone. Two other studies using a murine tibia loading model (21,22) have shown cancellous bone to respond to mechanical stimuli, however the reported effects were not as pronounced. Souza et al (21) was unable to show a significant anabolic effect between loading groups when loading 8 week old B6 mice, however a 37% increase in trabecular BV/TV was achieved when combining the data from all loading groups. Furthermore when applying the same loading regimes to 12 and 20 week old mice trabecular bone mass was shown to decline. In another study Fritton et al (22) reported similar 15 % increases in tibial trabecular BV/TV for two groups of female B6 mice (10 weeks of age). These mice were loaded for 2 weeks and 6

weeks using the same mechanical signal. As a reminder the increases seen in trabecular BV/TV in this loading study were 10% and 25% for load amplitudes of 4N and 8N respectively.

It is also the first time that loaded trabecular bone has been analysed in detail such that marked regional differences in bone formation have been indentified. This attribute indicates the presence of a diverse micromechanical environment which, when combined with the validated micro-finite element model (23), could be used to further our understanding of the underlying mechanical parameter(s) regulating trabecular bone formation and maintenance. The precise characterization of the mechanical signal responsible for load induced bone adaptation has been attempted in a few studies using rat and sheep models (29,30). However, owing to the size of these bones micro finite element models are only able to represent a small volume of the loaded bone. Consequently, the accuracy of the finite model is brought into question as important loading pathways are neglected and boundary conditions have to be approximated. This is not the case with the model presented here.

Despite being less pronounced, cortical bone formation was also shown to be dose dependent by micro-CT in the B6 strain. Although not significant ($P = 0.06$), global BV was shown to linearly/exponentially increase with load. A load induced anabolic effect was confirmed at a local level for a load of 8N, where significant group-region interaction terms were reported for both BV/TV_{Ct} and BV_{Ct}. Regional increases in Ct.Th followed a similar pattern to those described by BV_{Ct}. The increases in both B6 BV_{Ct} and Ct.Th, coupled with the non-significant increases in both MV and TV_{Ct} makes it difficult to draw any conclusions regarding the modality of remodelling at cortical sites. Rather than just simply depositing new bone on either or both of the cortical surfaces (endosteal and periosteal) it appears that a subtle thickening of the cortical shell is accompanied by both internal and external volumetric expansion, i.e. an increase in cross sectional moment of area. From an engineering perspective this would clearly accommodate the

optimal support of increased axial loads. Such a modality would require some kind of radial shift where greater periosteal bone formation rates are accompanied by resorption at endostial sites. This mechanism is not supported by histomorphometry which, for a load of 8N, shows a greater significant increase in bone formation at endosteal cortical sites compared to a smaller and non significant increase at periosteal sites. The precise characterization of load induced morphology would therefore require more detailed studies which are longitudinal in nature and which employ three dimensional, in vivo imaging techniques (31,32).

With respect to the second hypothesis, the comparative lack of bone formation in the C3H strain as shown by micro-CT suggests that mechano-sensitivity is genotype dependent, furthermore comparison of B6 and C3H histomorphometry appears to suggest that the response of C3H mice lag that of B6 mice: Despite greater 3-dimensional changes in B6 mice, osteoblast recruitment, osteoblast activity and bone formation rates at periosteal cortical sites are shown to be higher for the C3H strain and similar at trabecular and endosteal-cortical sites. This apparent temporal lag again alludes to the possible role of fatigue based mechanisms for load induced bone remodelling which is a viable assumption given that C3H cortical and trabecular bone is shown to be both thicker and stiffer at vertebral sites (16,33). This latter point highlights a limitation of the study. It is feasible that for equivalent axial loads the micro strains induced in C3H strains are lower than those induced in B6 vertebrae, hence the lack of response observed in the C3H strain could be explained by a reduced mechanical stimulus rather than genetic differences. Nevertheless the data presented here are supported by several other loading studies which have shown a smaller mechano-sensitive effect in C3H mice despite higher levels of micro-strain. Kesevan et al (13) demonstrated that B6 mice were more receptive to mechanical loading compared to C3H mice when loading their tibias using a 4 point bending modality even though higher mechanical strains were induced in C3H mice. B6 cortical thickness was shown to

increase by 28% compared to <10 % in C3H mice, when loaded for 6 days/week over a period of 2 weeks (Peak force: 9N, frequency: 2Hz). A similar effect was shown by Robling et al (8) when loading B6 and C3H ulna. Cortical bone in C3H mice has been shown to have a higher osteogenic threshold (2392 με) compared to that for B6 (1769 με), furthermore once the osteogeneic threshold was exceeded cortical bone formation per unit increase in mechanical strain was significantly less for C3H mice.

This model presented has two further limitations. Firstly, at the end of the study the animals are at an age (19 weeks) which is just short of skeletal maturity (20 weeks) (34). It is therefore possible that load induced bone formation could be complicated by growth factors, an aspect which must be considered when using this model to elucidate the biochemical pathways associated with load induced bone formation. Secondly, owing to the cross sectional nature of the study we were unable to indentify the exact spatial and temporal patterns of bone remodelling. However, this would be possible with the application of in vivo imaging technologies (31,32), a technology which is particularly suited to the imaging of caudal vertebrae given their accessible anatomical location. Furthermore, when combined with 'individualized' finite element models (23), in vivo imaging would also permit a more accurate characterization of the relationship between the mechanical environment and bone formation.

Conclusion

In performing this study we have demonstrated that we can surgically insert stainless steel pins into the C4 and C6 vertebrae of both B6 and C3H mice, we have also shown that we can accurately apply dynamic mechanical loads to their C5 vertebrae for a sustained period of time, whilst inducing a significant dose response in the cortical and trabecular bone of B6 mice. We have also provided strong evidence that the mechano-sensitivities for both cortical and trabecular

bone are genetically determined. The availability of this approach provides an alternative to the tibia loading model thus affording opportunities to explore site specific mechano-sensitivity in both cortical and trabecular bone. Moreover, the local variation of load induced bone trabecular bone formation will allow us to gain further insight into the underlying mechanical parameters and molecular process governing bone formation when combined with in vivo imaging technologies, finite element analysis and suitable methods of biochemical analysis.

Figure legends:

FIG. 1: (A) Fluoroscopic image of a mouse, graphically edited to show the location and form of the stainless steel pins once they have been surgically inserted. The mechanical signal is applied to the distal pin whilst the proximal pin is clamped. (B) One loading axis of the Caudal Vertebra Axial Compression Device (CVAD).

FIG. 2: (A) Digital image of a whole B6 vertebra (C5) showing cortical and trabecular components. (B) B6 trabecular bone subdivided into 15 overlapping regions (1_{Tb}–15_{Tb}). (C) B6 cortical shell subdivided into 15 overlapping regions (1_{Ct}–15_{Ct}) which match those defining the 15 trabecular regions.

FIG. 3: (A) Percentage increase in global BV/TV_{Tb} for B6 and C3H mice loaded at 0N, 2N, 4N and 8N. [a] Significantly different 0N loading group of same biological strain ($P < 0.01$). [b] Significant inter-strain difference ($P < 0.01$). (B) Mean regional variation of Tb.N (absolute values) as measured by $B6_{0N}$ and $B6_{8N}$ loading groups, standard errors shown. (C) Mean regional variation of BV/TV_{Tb} (absolute values) as measured by $C3H_{0N}$ and $C3H_{8N}$ loading groups. All Error bars show the standard error.

FIG. 4: Visual comparison of loaded caudal vertebrae from both B6 and C3H mice. The grey-scale images show transverse sections from the uppermost slice of region 3_{Tb}. Samples with median BV/TV_{Tb} from each loading groups are displayed.

FIG. 5: Bar charts showing the change of Md.Pm/Pm, MAR and BFR/Pm with load for B6and C3H mice at trabecular (A) periosteal-cortical (B) and endosteal-cortical (C) sites.

[a] Significantly different to the 0N loading group of same strain ($P < 0.05$). [b] Significantly different to C3H strain. [c] Almost significantly different to 0N loading group of same biological strain ($P < 0.06$). Error bars show standard deviation.

FIG. 6: (A) Percentage increase in global BV_{Ct} for B6 and C3H mice loaded at 0N, 2N, 4N and 8N, standard errors shown. (B) Mean regional variation of BV_{Ct} (absolute values) as measured by $B6_{0N}$ and $B6_{8N}$ loading groups. [b] Significantly different to C3H strain ($P < 0.05$). [c] Almost significantly different to 0N loading group of same biological strain ($P < 0.06$). Standard errors are shown.

References

1. Evans WJ 1998 Exercise and nutritional needs of elderly people: effects on muscle and bone. Gerodontology **15**(1)**:**15-24.
2. Duncan RL, Turner CH 1995 Mechanotransduction and the functional response of bone to mechanical strain. Calcif Tissue Int **57**(5)**:**344-58.
3. Biewener AA, Fazzalari NL, Konieczynski DD, Baudinette RV 1996 Adaptive changes in trabecular architecture in relation to functional strain patterns and disuse. Bone **19**(1)**:**1-8.
4. Rubin CT, Lanyon LE 1985 Regulation of bone mass by mechanical strain magnitude. Calcif Tissue Int **37**(4)**:**411-7.
5. Frost HM 1987 The mechanostat: a proposed pathogenic mechanism of osteoporoses and the bone mass effects of mechanical and nonmechanical agents. Bone Miner **2**(2)**:**73-85.
6. Albright J 1987 The scientific basis of orthopaedics, 2 ed. Appleton-Century Crofts, New York.
7. Marcus R 1995 Relationship of age-related decreases in muscle mass and strength to skeletal status. J Gerontol A Biol Sci Med Sci **50 Spec No:**86-7.
8. Robling AG, Turner CH 2002 Mechanotransduction in bone: genetic effects on mechanosensitivity in mice. Bone **31**(5)**:**562-9.
9. Kuruvilla SJ, Fox SD, Cullen DM, Akhter MP 2008 Site specific bone adaptation response to mechanical loading. J Musculoskelet Neuronal Interact **8**(1)**:**71-8.
10. Akhter MP, Cullen DM, Pedersen EA, Kimmel DB, Recker RR 1998 Bone response to in vivo mechanical loading in two breeds of mice. Calcif Tissue Int **63**(5)**:**442-9.
11. Xing W, Baylink D, Kesavan C, Hu Y, Kapoor S, Chadwick RB, Mohan S 2005 Global gene expression analysis in the bones reveals involvement of several novel genes and pathways in mediating an anabolic response of mechanical loading in mice. J Cell Biochem **96**(5)**:**1049-60.
12. Lau KH, Kapur S, Kesavan C, Baylink DJ 2006 Up-regulation of the Wnt, estrogen receptor, insulin-like growth factor-I, and bone morphogenetic protein pathways in C57BL/6J osteoblasts as opposed to C3H/HeJ osteoblasts in part contributes to the differential anabolic response to fluid shear. J Biol Chem **281**(14)**:**9576-88.
13. Kesavan C, Mohan S, Oberholtzer S, Wergedal JE, Baylink DJ 2005 Mechanical loading-induced gene expression and BMD changes are different in two inbred mouse strains. J Appl Physiol **99**(5)**:**1951-7.
14. Kodama Y, Umemura Y, Nagasawa S, Beamer WG, Donahue LR, Rosen CR, Baylink DJ, Farley JR 2000 Exercise and mechanical loading increase periosteal bone formation and whole bone strength in C57BL/6J mice but not in C3H/Hej mice. Calcif Tissue Int **66**(4)**:**298-306.
15. Koller DL, Schriefer J, Sun Q, Shultz KL, Donahue LR, Rosen CJ, Foroud T, Beamer WG, Turner CH 2003 Genetic effects for femoral biomechanics, structure, and density in C57BL/6J and C3H/HeJ inbred mouse strains. J Bone Miner Res **18**(10)**:**1758-65.
16. Turner CH, Hsieh YF, Muller R, Bouxsein ML, Baylink DJ, Rosen CJ, Grynpas MD, Donahue LR, Beamer WG 2000 Genetic regulation of cortical and trabecular bone strength and microstructure in inbred strains of mice. J Bone Miner Res **15**(6)**:**1126-31.
17. Beamer WG, Shultz KL, Donahue LR, Churchill GA, Sen S, Wergedal JR, Baylink DJ, Rosen CJ 2001 Quantitative trait loci for femoral and lumbar vertebral bone mineral

density in C57BL/6J and C3H/HeJ inbred strains of mice. J Bone Miner Res **16**(7)**:**1195-206.
18. Kesavan C, Mohan S, Srivastava AK, Kapoor S, Wergedal JE, Yu H, Baylink DJ 2006 Identification of genetic loci that regulate bone adaptive response to mechanical loading in C57BL/6J and C3H/HeJ mice intercross. Bone **39**(3)**:**634-43.
19. Guo XE, Eichler MJ, Takai E, Kim CH 2002 Quantification of a rat tail vertebra model for trabecular bone adaptation studies. J Biomech **35**(3)**:**363-8.
20. Chambers TJ, Evans M, Gardner TN, Turner-Smith A, Chow JW 1993 Induction of bone formation in rat tail vertebrae by mechanical loading. Bone Miner **20**(2)**:**167-78.
21. De Souza RL, Matsuura M, Eckstein F, Rawlinson SC, Lanyon LE, Pitsillides AA 2005 Non-invasive axial loading of mouse tibiae increases cortical bone formation and modifies trabecular organization: a new model to study cortical and cancellous compartments in a single loaded element. Bone **37**(6)**:**810-8.
22. Fritton JC, Myers ER, Wright TM, van der Meulen MC 2005 Loading induces site-specific increases in mineral content assessed by microcomputed tomography of the mouse tibia. Bone **36**(6)**:**1030-8.
23. Webster DJ, Morley PL, van Lenthe GH, Muller R 2008 A novel in vivo mouse model for mechanically stimulated bone adaptation--a combined experimental and computational validation study. Comput Methods Biomech Biomed Engin **11**(5)**:**435-41.
24. Hilderbrand T 1999 Direct three-demensional morphometric analysis of human cancellous bone: microstructural data from spine, femur, iliac crest and calcaneus. J Bone Miner Res **14:**1167-1174.
25. Kohler T, Stauber M, Donahue LR, Muller R 2007 Automated compartmental analysis for high-throughput skeletal phenotyping in femora of genetic mouse models. Bone **41**(4)**:**659-67.
26. Parfitt AM 1988 Bone histomorphometry: proposed system for standardization of nomenclature, symbols, and units. Calcif Tissue Int **42**(5)**:**284-6.
27. Bronckers AL, Goei W, Luo G, Karsenty G, D'Souza RN, Lyaruu DM, Burger EH 1996 DNA fragmentation during bone formation in neonatal rodents assessed by transferase-mediated end labeling. J Bone Miner Res **11**(9)**:**1281-91.
28. Verborgt O, Gibson GJ, Schaffler MB 2000 Loss of osteocyte integrity in association with microdamage and bone remodeling after fatigue in vivo. J Bone Miner Res **15**(1)**:**60-7.
29. Kim CH, Takai E, Zhou H, von Stechow D, Muller R, Dempster DW, Guo XE 2003 Trabecular bone response to mechanical and parathyroid hormone stimulation: the role of mechanical microenvironment. J Bone Miner Res **18**(12)**:**2116-25.
30. Judex S, Boyd S, Qin YX, Turner S, Ye K, Muller R, Rubin C 2003 Adaptations of trabecular bone to low magnitude vibrations result in more uniform stress and strain under load. Ann Biomed Eng **31**(1)**:**12-20.
31. Boyd SK, Davison P, Muller R, Gasser JA 2006 Monitoring individual morphological changes over time in ovariectomized rats by in vivo micro-computed tomography. Bone **39**(4)**:**854-62.
32. F. M. Lambers, G. Kuhn, F. A. Gerhard, R. Müller 2009 In vivo micro computed tomography allows monitoring of load induced microstructural bone adaptation. Bone (44(S2):in press).
33. Akhter MP, Fan Z, Rho JY 2004 Bone intrinsic material properties in three inbred mouse strains. Calcif Tissue Int **75**(5)**:**416-20.

34. Brodt MD, Ellis CB, Silva MJ 1999 Growing C57Bl/6 mice increase whole bone mechanical properties by increasing geometric and material properties. J Bone Miner Res **14**(12)**:**2159-66.

Figure

Table 1

TABLE 1. MEAN ABSOLUTE VALUES FOR GLOBAL MORPHOLOGICAL PARAMETERS SPECIFIC TO TRABECULAR AND CORTICAL COMPONENTS FOR B6 AND C3H LOADING GROUPS

	Trabecular bone (T_b)					Cortical bone (C_t)				
Group	BV/TV (%)	BV (mm^3)	TV (mm^3)	Tb.Th (μm)	Tb.N (mm^{-1})	BV/TV (%)	BV (mm^3)	TV (mm^3)	Ct.Th (μm)	MV (mm^3)
$B6_{0N}$	20.9 ± 0.62 [b]	0.61 ± 0.02 [b]	2.96 ± 0.07 [b]	76.7 ± 2.21 [b]	2.95 ± 0.03 [b]	36.5 ± 0.72 [b]	2.01 ± 0.06 [b]	5.49 ± 0.12 [b]	129.9 ± 2.57 [b]	3.48 ± 0.09 [b]
$B6_{2N}$	20.5 ± 0.83	0.63 ± 0.03	3.11± 0.05	78.5 ± 2.19	2.85 ± 0.05	35.7 ± 0.73	2.03 ± 0.06	5.68 ± 0.08	129.0 ± 2.84	3.65 ± 0.05
$B6_{4N}$	22.5 ± 0.43	0.66 ± 0.01	2.95 ± 0.06	78.7 ± 1.39	3.05 ± 0.08	37.3 ± 0.48	2.09 ± 0.04	5.62 ± 0.09	131.9 ± 1.71	3.52 ± 0.06
$B6_{8N}$	26.3 ± 0.73 [a]	0.80 ± 0.04 [a]	3.02 ± 0.08	93.5 ± 1.63 [a]	3.03 ± 0.08	38.4 ± 0.23	2.23 ± 0.06 [c]	5.82 ± 0.15	136.9 ± 1.42	3.58 ± 0.09
$C3H_{0N}$	11.9 ± 0.26	0.29 ± 0.008	2.48 ± 0.05	91.5 ± 1.39	1.99 ± 0.06	50.5 ± 0.37	2.98 ± 0.06	5.91± 0.10	185.9 ± 1.48	2.92 ± 0.05
$C3H_{2N}$	12.4 ± 0.41	0.31 ± 0.01	2.46 ± 0.03	92.5 ± 1.60	1.96 ± 0.04	51.2 ± 0.49	3.07 ± 0.05	6.01 ± 0.06	187.0 ± 2.45	2.93 ± 0.04
$C3H_{4N}$	11.7 ± 0.40	0.29 ± 0.01	2.53 ± 0.06	92.7 ± 1.49	2.00 ± 0.07	50.2 ± 0.64	3.02 ± 0.09	6.02 ± 0.15	185.6 ± 2.96	2.99 ± 0.08
$C3H_{8N}$	13.5 ± 0.64 [c]	0.33 ± 0.01	2.48 ± 0.06	98.7 ± 3.42	1.99 ± 0.09	50.1 ± 1.03	2.98 ± 0.07	5.94 ± 0.08	182.4 ± 4.89	2.96 ± 0.07

[a] Significant relative to 0N loading group of same biological strain ($P < 0.001$).

[b] Significant relative to $C3H_{0N}$ ($P < 0.001$).

[c] Almost significant relative to 0N loading group of same biological strain ($P < 0.06$)

Fig 1

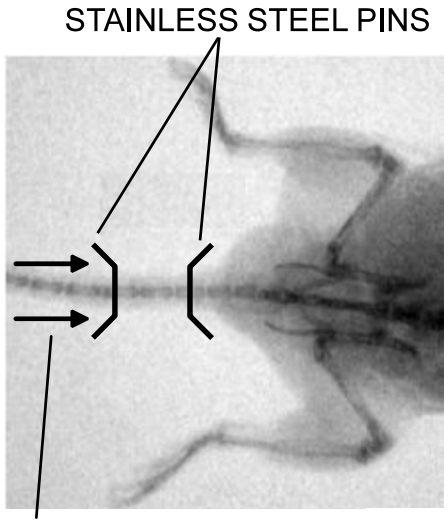
STAINLESS STEEL PINS
APPLIED MECHANICAL SIGNAL

A

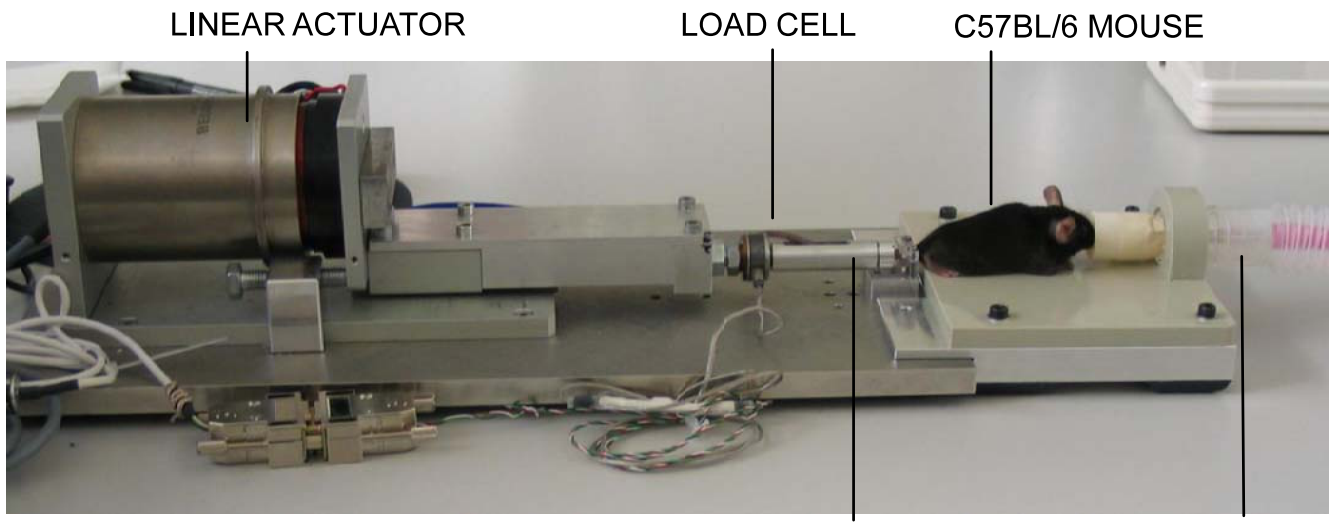
LINEAR ACTUATOR
LOAD CELL
C57BL/6 MOUSE
APPLICATOR
ANESTHETIZING TUBE

B

Fig 2

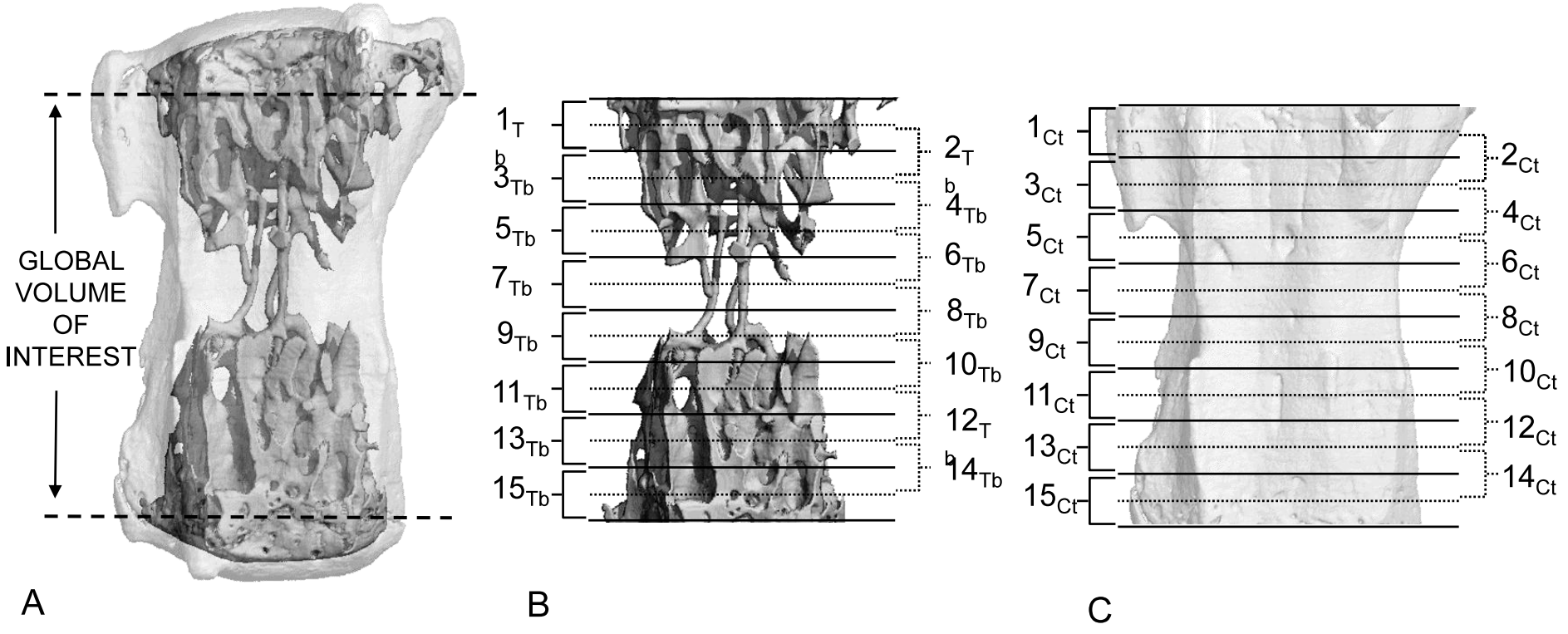
GLOBAL
VOLUME
OF
INTEREST
1T
b
3Tb
5Tb
7Tb
9Tb
11Tb
13Tb
15Tb
2T
b
4Tb
6Tb
8Tb
10Tb
12T
b
14Tb
1Ct
3Ct
5Ct
7Ct
9Ct
11Ct
13Ct
15Ct
2Ct
4Ct
6Ct
8Ct
10Ct
12Ct
14Ct
A
B
C

Fig 3

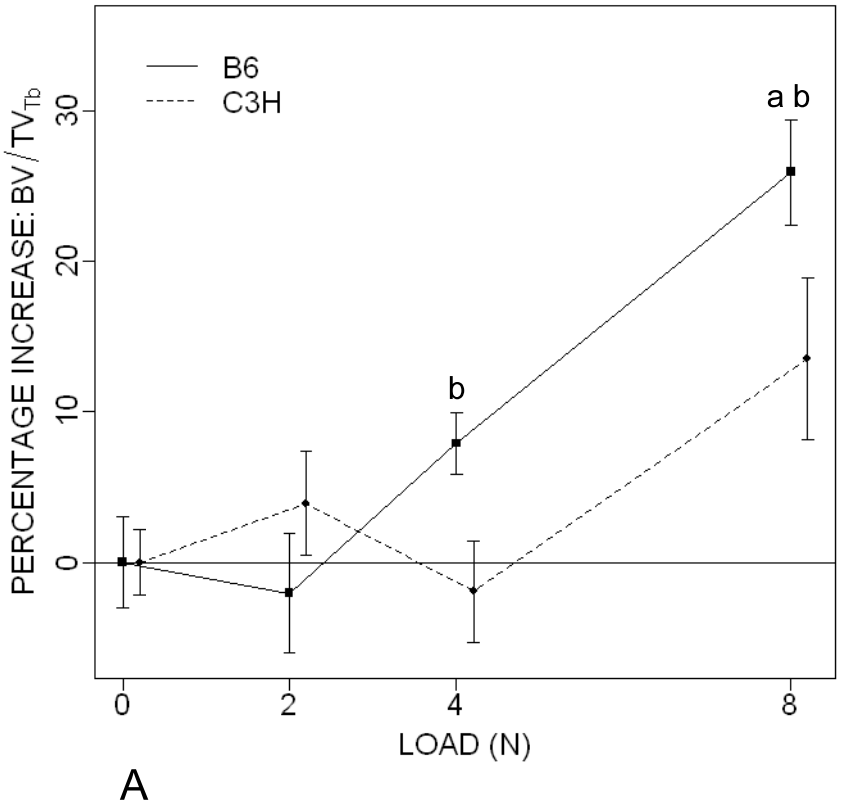
B6
C3H
a b
b
PERCENTAGE INCREASE: BV / TV$_{Tb}$
0
10
20
30
0
2
4
8
LOAD (N)

A

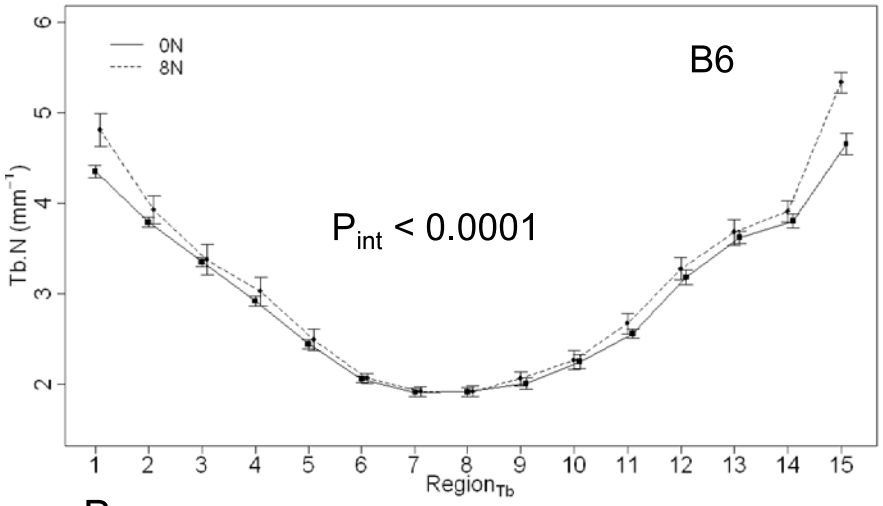
0N
8N
B6
P$_{int}$ < 0.0001
Tb.N (mm^{-1})
2
3
4
5
6
1
2
3
4
5
6
7
8
9
10
11
12
13
14
15
Region$_{Tb}$

B

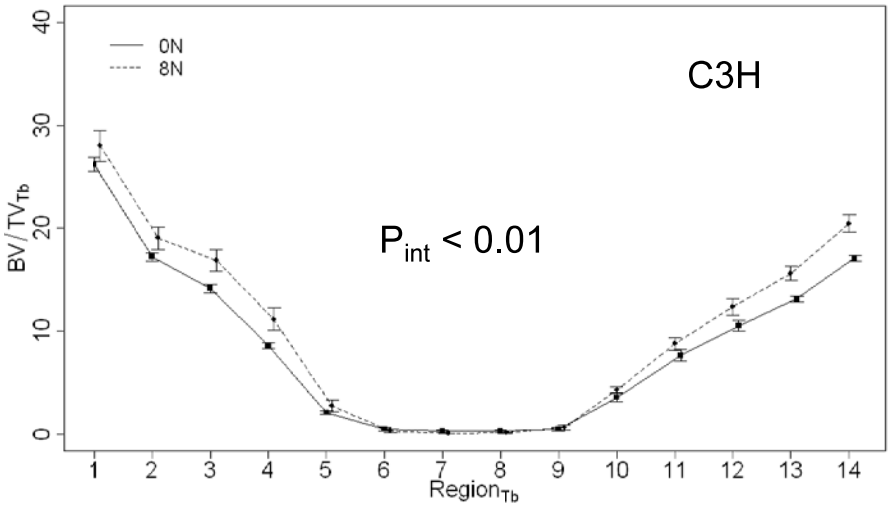
0N
8N
C3H
P$_{int}$ < 0.01
BV / TV$_{Tb}$
0
10
20
30
40
1
2
3
4
5
6
7
8
9
10
11
12
13
14
Region$_{Tb}$

C

Fig 4

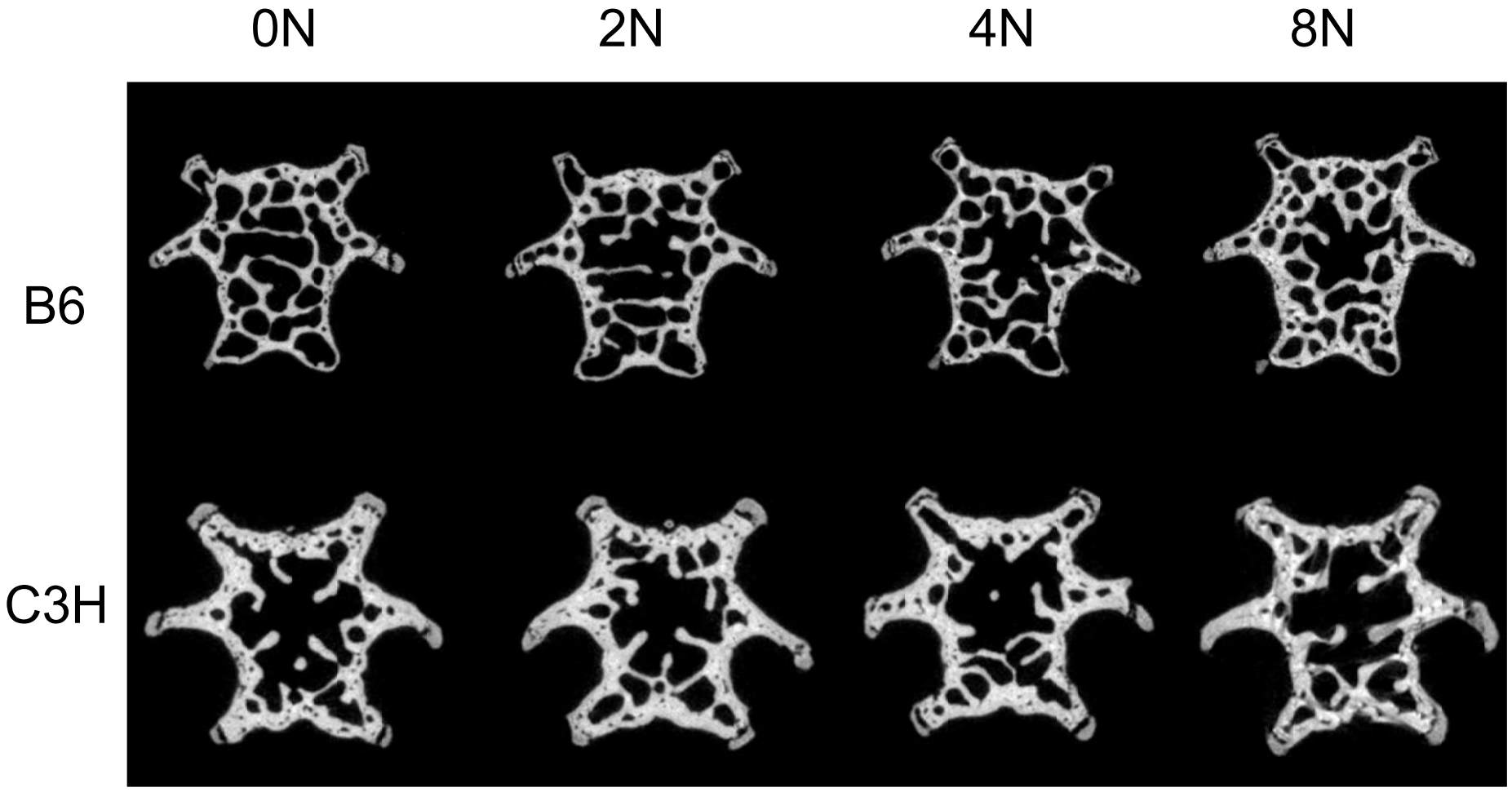
0N
2N
4N
8N
B6
C3H

Fig 5a, b, c

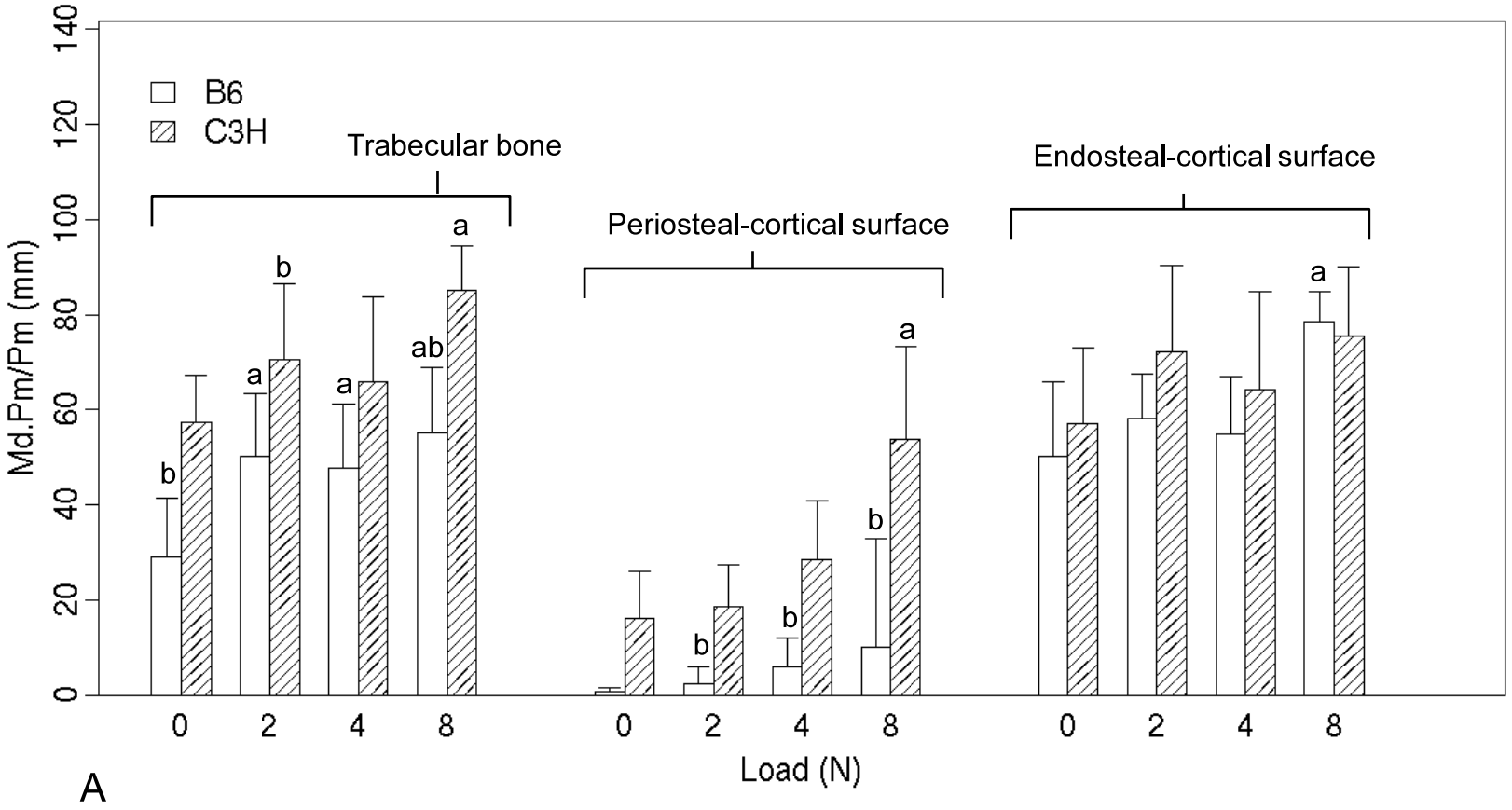
B6
C3H
Trabecular bone
Periosteal-cortical surface
Endosteal-cortical surface
Md.Pm/Pm (mm)
0
20
40
60
80
100
120
140
b
a
b
a
a
ab
a
b
b
b
a
a
b
a
0
2
4
8
0
2
4
8
0
2
4
8
Load (N)

A

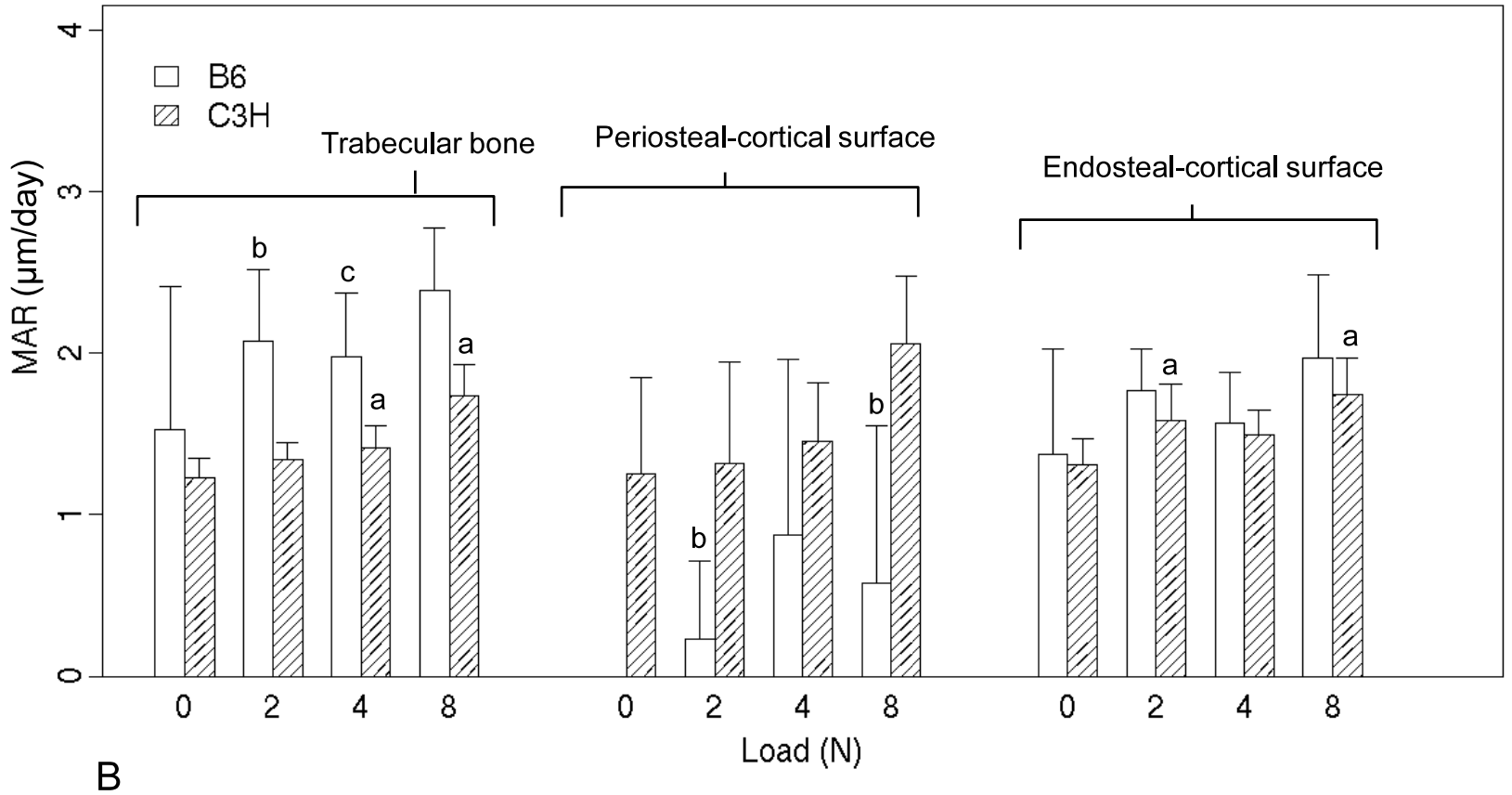
B6
C3H
Trabecular bone
Periosteal-cortical surface
Endosteal-cortical surface
MAR (μm/day)
0
1
2
3
4
b
c
a
b
a
b
a
0
2
4
8
Load (N)

B

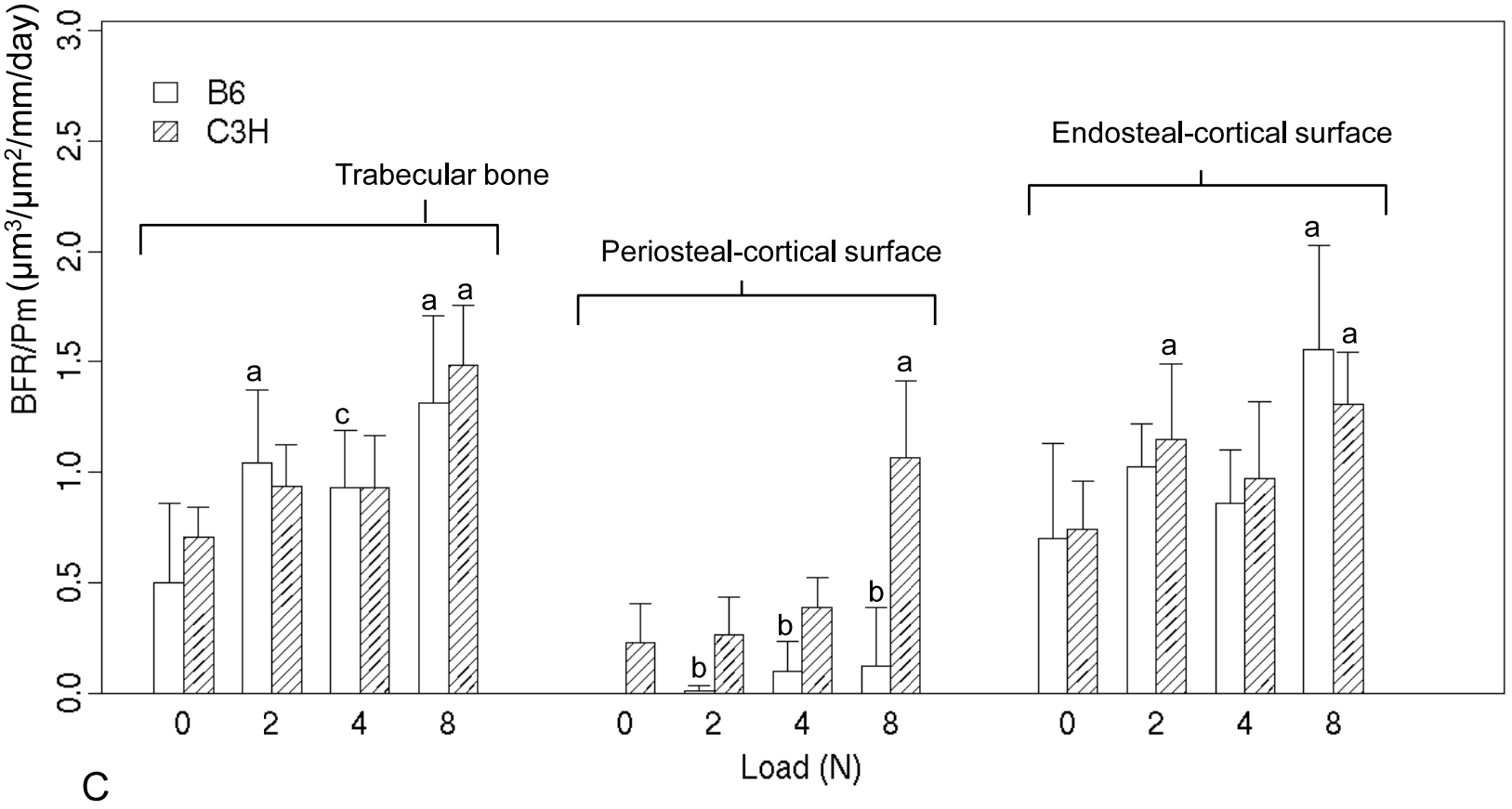
BFR/Pm (μm³/μm²/mm/day)
0.0
0.5
1.0
1.5
2.0
2.5
3.0
B6
C3H
Trabecular bone
Periosteal-cortical surface
Endosteal-cortical surface
a
a
c
a
a
b
b
a
a
a
a
0
2
4
8
0
2
4
8
0
2
4
8
Load (N)

C

Fig 6

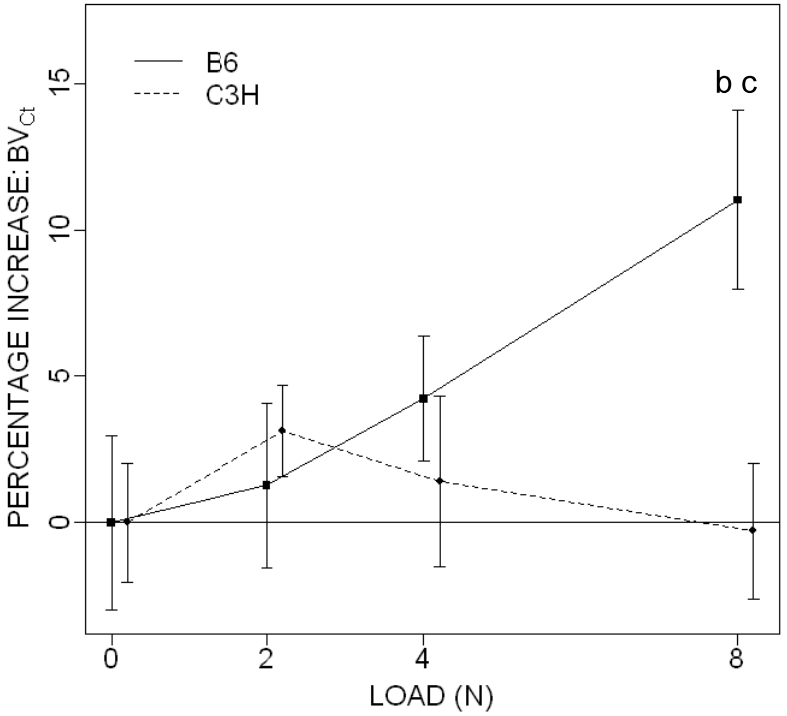
B6
C3H
b c
PERCENTAGE INCREASE: BV_{Ct}
0
5
10
15
0
2
4
8
LOAD (N)

A

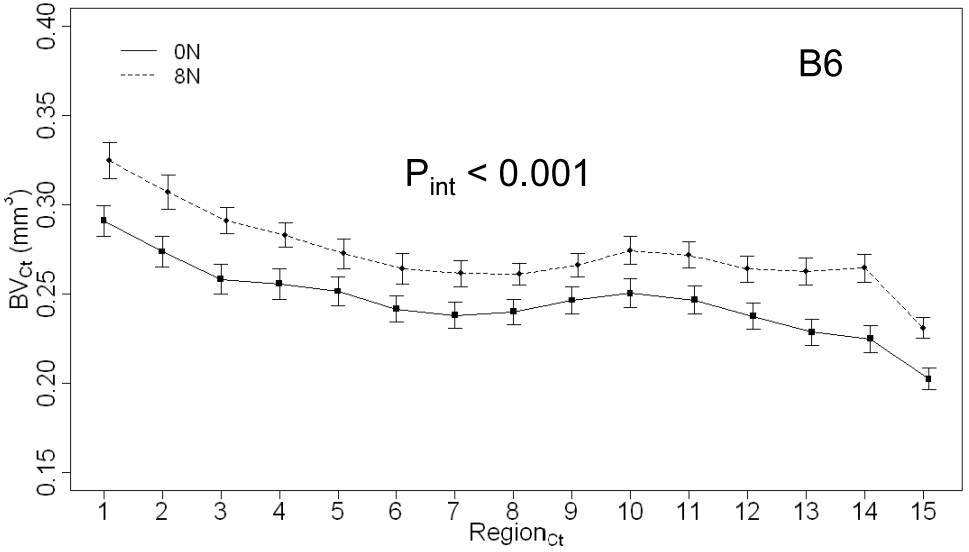
0N
8N
B6
$P_{int} < 0.001$
BV_{Ct} (mm^3)
0.15
0.20
0.25
0.30
0.35
0.40
1
2
3
4
5
6
7
8
9
10
11
12
13
14
15
$Region_{Ct}$

B